Crystal chemistry of M II M' IV (PO 4) 2 double monophosphates

Damien Bregiroux, Karin Popa, Gilles Wallez

Review paper

Crystal chemistry of $M^{II}M'^{IV}(PO_4)_2$ double monophosphates

Damien Bregiroux,[1] Karin Popa,[2] and Gilles Wallez[3,4]*

[1] Sorbonne Universités, UPMC Univ Paris 06, CNRS, Collège de France, Laboratoire de Chimie de la Matière Condensée de Paris, 11 place Marcelin Berthelot, 75005 Paris, France.

[2] "Al.I. Cuza" University, Department of Chemistry, 11-Carol I Blvd., 700506 Iasi, Romania

[3] Institut de Recherche de Chimie Paris (IRCP), CNRS – Chimie ParisTech – Paris Sciences et Lettres PSL UMR8247, 11 rue Pierre et Marie Curie, 75005 Paris, France

[4] Sorbonne Universités, UPMC Univ Paris 06

[*]Corresponding author: damien.bregiroux@upmc.fr

Tel. : +33 (0)1 44 27 15 28

Fax. : +33 (0)1 44 27 15 04

Abstract

$M^{II}M'^{IV}(PO_4)_2$ compounds have been extensively studied for several decades for their potential applications in the field of several domains such as matrices for actinides conditioning, phosphors… In this paper, the relationships between composition and crystal structure of these compounds are established. A review of the various processes used for the synthesis of these compounds is also proposed, as well as their most reported properties. $M^{II}M'^{IV}(PO_4)_2$ structures stem from two different archetypes: the cheralite and the yavapaiite structures, with some exceptions that are also described in this article. The ratio of the cations

radii appears to be the most relevant parameter. The high ratio between the ionic radii of the divalent and tetravalent cations in yavapaiite derivates results in the ordering of these cations into well-differentiated polyhedra whereas cheralite is the only non-ordered structure encountered for $M^{II}M'^{IV}(PO_4)_2$ compounds.

Keywords

Phosphate, Cheralite, Yavapaiite, Crystal structure

1. Introduction

Anhydrous $M^{II}M'^{IV}(PO_4)_2$ (M^{II}= Cd, Ca, Sr, Pb, Ba; M'^{IV}= Ge, Ti, Mo, Sn, Hf, Zr, Pu, Np, U, Th) are double monophosphates in which metal-containing polyhedra are linked to phosphate tetrahedra by faces, edges or corners. Among them, compounds with the cheralite structure are the only ones that can be found as natural crystals [1]. Most of the studies carried out on this family of compounds addressed to the actinides phosphates [2-8], but it is also an interesting field of investigation as ionic conductors [9], catalysts and ion exchangers [10], luminescent materials and UV-emitting X-ray phosphors [11-13]. Some of them are also likely to occur in the residuals of the phosphate-based treatment processes of nuclear wastes [14]. In a previous review, Brandel and Dacheux classified phosphate compounds according to the charge of the framework [15,16]. Thus, all the inorganic phosphates can be classified on the basis of the general framework $[(M^h)_m(A^q)_p]^k$, with k = hm + pq. Applied to tetravalent M'^{IV} cations the various phosphate anions (A^q) could be $H_2PO_4^-$, HPO_4^{2-}, PO_4^{3-}, $P_2O_7^{4-}$, PO_3^-, etc. Three main families result from this formula: uncharged compounds (k= 0), phosphates with cationic framework (k > 0) and with anionic framework (k < 0). $M^{II}M'^{IV}(PO_4)_2$ compounds are part of the sub-group of phosphates of the $(M^n)_xM'(PO_4)_2$ type (q = -3 and m = 1, anionic framework), in which $(M^n)_x$ is a divalent Cd, Ca, Sr, Pb, Ba, so x = 1. Such

phosphates can be considered as derivatives of hydrogen phosphates $M'^{IV}(HPO_4)_2$, where the divalent cation replaces both protons. More recently, Locock proposed a classification based on the coordination number of the tetravalent cation (usually, an actinide element) [6]. As the coordination environments of the actinides differ with valence state, the author found convenient to discuss the compounds of the lower valence-state actinides separately from those of the higher valence-states.

Insofar as the potential applications of this family of compounds involve a wide spectrum of cations (transition, lanthanides, actinides and s- and p-block elements), it is necessary to establish the relationship between the cation and the resulting structure, including its thermal behavior. For several years, much information has been published on the crystal chemistry of the $M^{II}M'^{IV}(PO_4)_2$ compounds. This paper aims to review the relationships between composition and crystal structure of these compounds and to propose a comprehensive classification. A review of the various processes used for the synthesis of these compounds is also proposed, as well as their most reported properties.

2. Synthesis

Table 1 reports different protocols described in the literature for the synthesis of $M^{II}M'^{IV}(PO_4)_2$ compounds. Note that authors did not always specify purity of the final products. In most cases, the synthesis was achieved by solid-state route from $M'^{IV}O_2$ oxide, $M^{II}CO_3$ carbonate and di-ammonium hydrogen phosphate $(NH_4)_2HPO_4$ (or ammonium di-hydrogen phosphate $NH_4H_2PO_4$). The synthesis temperature was classically in the range of 1373-1673 K for several hours. For shorter reaction time or lower temperature, $M'O_2$, $M'P_2O_7$ or even $M_3(PO_4)_2$ were detected as additional phases [17]. Several authors used an excess of phosphate precursor (5 to 25 wt. %) in order to avoid the presence residual $M'O_2$ [4,18-22]. The only example of a $M^{II}M'^{IV}(PO_4)_2$ compound obtained at ambient pressure by wet

chemistry route was reported by Wallez *et al.* for the synthesis of $BaTh(PO_4)_2$. The synthesis of $BaTh(PO_4)_2$ by solid state reaction always leads to significant residual ThO_2 and β-thorium phosphate diphosphate (β-TPD, $Th_4(PO_4)_4(P_2O_7)$), both known for their high thermal stability [23]. Most of time, except for actinide compounds, $CaM'^{IV}(PO_4)_2$ is obtained by using a two-step protocol: perovskite $CaM'O_3$ is firstly synthesized at high temperature before being reacted with $NH_4H_2PO_4$ [10,13,24]. Several authors obtained $M^{II}M'^{IV}(PO_4)_2$ compounds by hydrothermal route [25-28]. Some compounds can also be obtained as small single crystals, by high temperature single crystal growth method (HTSG) [29] or flux crystal growth [9,30,31]. Note that within the frame of this review, we obtained $PbSn(PO_4)_2$ by a classical solid state route at 1273 K from a mixture of $PbCO_3$, SnO_2 and $NH_4H_2PO_4$, whereas the only elaboration route reported in the literature dealt with single crystals [9]. The melting point of this compound was determined to be around 1298 K.

Table 1

Review of the different synthesis routes used to obtain $M^{II}M'^{IV}(PO_4)_2$ compounds

Composition	**Reaction**	**Thermal treatment**	**Ref.**
$BaM'(PO_4)_2$ (*M'* = Ge, Ti, Sn, Zr)	$BaCO_3 + M'O_2 + 2(NH_4)_2HPO_4$	1373 K – several days	[32]
$BaM'(PO_4)_2$ (*M'* = Zr and Hf)	$BaCO_3 + M'O_2 + 2(NH_4)_2HPO_4$ (+wt. 25% excess)	1473 K – 10 h	[4]
$BaMo(PO_4)_2$	Single crystal growth in Mo-phosphate flux from a mixture of $BaCO_3$, $(NH_4)_2HPO_4$ and MoO_3	1173 K – 12 h in evacuated sealed ampoule then quenched to RT	[31]
$BaNp(PO_4)_2$	$BaCO_3 + NpO_2 + 2(NH_4)_2HPO_4$ (+wt. 5% excess)	1381 K – 10 h + grinding + 1485 K – 10 h, Ar	[18]
$BaTh(PO_4)_2$	Precipitation at room temperature from a mixture of $Th(NO_3)_4{\cdot}5H_2O$, $Ba(NO_3)_2$ and $NH_4H_2PO_4$	Slow heating up to 873 K + 1523 K – 24 h	[18]

$BaZr_{1-x}Hf_x(PO_4)_2$	$BaCO_3 + (1-x)ZrO_2 + xHfO_2 + 2NH_4H_2PO_4$	1373 K – 12 h	[12]
$CaM'(PO_4)_2$ (M' = Th, Np)	$CaCO_3 + M'O_2 + 2(NH_4)_2HPO_4$ (10% excess)	1523 K – 100 h (M' = Th) 1473 K – 20 h (M'= Np)	[20]
$CaNp_{1-x}Pu_x(PO_4)_2$	$(1-x)NpO_2 + xPuO_2 + CaCO_3 + 2(NH_4)H_2PO_4$	1473 K	[33]
$CaTh(PO_4)_2$	$CaCO_3 + ThO_2 + 2(NH_4)_2HPO_4$ (10% excess)	1523 K – 100 h	[21]
$CaTh(PO_4)_2$	Hydrothermal precipitation from a mixture of $Th(OH)_4$, $Ca(OH)_2$ and H_3PO_4	1053 K – 200 MPa	[28]
$CaTh_{1-x}U_x(PO_4)_2$	$Ca(HPO_4)\cdot 2H_2O + (1-x)ThO_2 + xUO_2 + NH_4H_2PO_4$	Several successive room temperature mechanical grinding / heating at 1473 K – 10 h, Ar cycles	[34]
$CaU(PO_4)_2$	Hydrothermal precipitation from a mixture of $UO_{2.12}$, $Ca(OH)_2$ and H_3PO_4	773 K – 200 MPa	[26]
$CaU(PO_4)_2$	Hydrothermal precipitation from a mixture of $UO_{2.12}$, CaO and H_3PO_4	1053 K – 200 MPa	[27]
$CaZr(PO_4)_2$:*RE* (*RE* = Eu^{3+}, Tb^{3+} and Tm^{3+})	(a) $CaCO_3 + ZrO_2$ + *RE* oxide → $CaZrO_3$:*RE* (b) pellets of $CaZrO_3$:*RE* + $2NH_4H_2PO_4$	(a) 1573 K – 2 h (b) 1473 K – 10 h	[13]
$MTh(PO_4)_2$ (M = Ca, Cd, Sr, Pb and Ba)	Hydrothermal treatment of phosphate gels obtained by precipitation between aqueous solutions of M and Th nitrates or carbonates and $(NH_4)_2HPO_4$	1473 K, 24 h, 1 bar or 973 K, 7 days, 2500 bars	[25]
$MZr(PO_4)_2$ (M = Ca and Ba)	(a) $MCO_3 + ZrO_2 \rightarrow MZrO_3$ (b) pellets of $MZrO_3 + 2NH_4H_2PO_4$	(a) 1773 K – 1 h (b) 1573 K – 100 h (M =Ba) or 1473 K – 30 min (M =Ca) followed by quenching to room temperature	[10-24]
$PbGe(PO_4)_2$	Single crystal growth from a mixture of $PbCl_2$, GeO_2 and $NH_4H_2PO_4$ (1:20:133 mol.)	673 K – 1 day, then 1323 K – 2 days followed by cooling down to 1023 K at 3 $K.h^{-1}$ and down to 573 K at 5 $K.h^{-1}$	[35,36]

$PbM'(PO_4)_2$ (M' = Ge and Ti)	$PbO + M'O_2 + 2NH_4H_2PO_4$	1273 K – 2 days	[35]
$Pb_{1-x}Eu_xGe(PO_4)_2$	$(1-x)PbO + x/2Eu_2O_3 + GeO_2 + 2NH_4H_2PO_4$	1273 K – 24 h	[35]
$PbSn(PO_4)_2$	Single crystal growth in Sn-phosphate flux from a mixture of $PbCO_3$, SnO_2 and $NH_4H_2PO_4$	1373 K followed by a slow cooling (5 $K.h^{-1}$) to 1073 K	[9]
$PbZr(PO_4)_2$	Single crystal growth in Pb-phosphate flux: $ZrO_2 + 2.37PbO\text{-}P_2O_5$	1673 K – 20 h followed by very slow cooling (3.2 $K.h^{-1}$)	[30]
$SrNp(PO_4)_2$	$Sr(NO_3)_2 + NpO_2 + 2(NH_4)_2HPO_4$ (20% excess)	1381 K – 24 h + 1485 K – 24 h, Ar	[22]
$SrTh(PO_4)_2$	$SrCO_3 + ThO_2 + 2NH_4H_2PO_4$	673 K – 6 h + 1223 K – 48 h (purity not specified)	[37]
$SrTi(PO_4)_2$, $SrSn(PO_4)_2$ and $BaSn(PO_4)_2$	$SrCO_3$ (or $BaCO_3$) + TiO_2 (or SnO_2)+ $2NH_4H_2PO_4$	Single crystal growth by HTSG method in open air	[29]
$Sr_{1-x}Ba_xZr(PO_4)_2$	$(1-x)SrCO_3 + xBaCO_3 + ZrO_2 + 2NH_4H_2PO_4$	1673 K – 5 h on pellets	[38]

3. Crystal structures

Fig. 1 reports the structures which can be obtained with the $M^{II}M'^{IV}(PO_4)_2$ formula. In all the figures of this paper, blue color refers to M^{IV} polyhedra, green color to M^{II} polyhedra (M^{II} and M^{IV} in the case of cheralite) and orange color to PO_4 tetrahedra. Note that the structures of some compounds were not published and were consequently assigned in this review to a structural domain on the basis of the X-ray diffraction pattern. As discussed later, the structures can be classified according to the two cations sizes (r_c, according to Shannon [39], or extrapolated) and stem from two different archetypes: the cheralite and the yavapaiite structures.

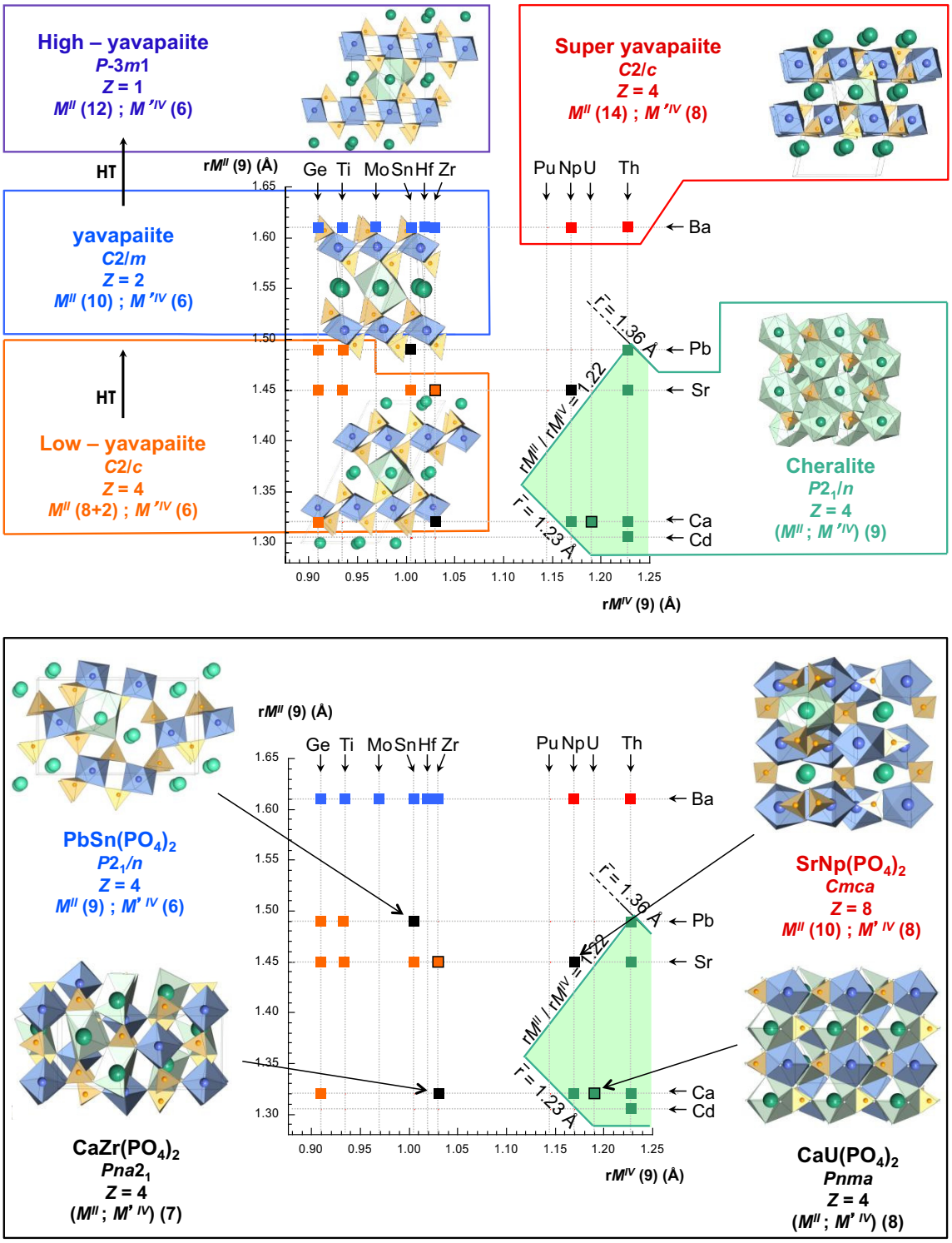

Fig. 1. Existing domains of $M^{II}M'^{IV}(PO_4)_2$ structures as a function of the M and M' ionic radii in nine-fold coordination: main structures (upper graph) and exceptions (lower graph). Numbers between brackets are the coordination number of M and M'.

3.1. The cheralite and yavapaiite structures

Reported for the first time by Bowie *et al.* in 1953 [40], the cheralite mineral, whose archetype is $CaTh(PO_4)_2$, is an analogue of monazite $CePO_4$, where Ce is replaced randomly by Ca and Th. Also named brabantite, it was described by Rose *et al.* in 1980 [41]. The name "brabantite" was recently replaced by "cheralite" according to Linthout paper published in 2007 [42]. Cheralite compounds crystallize in the monoclinic $P2_1/n$ space group ($Z = 4$) [43]. This structure consists of chains made up by alternating edges-linked irregular nine-fold-coordinated *M*/*M'* cations and distorted tetrahedral phosphate groups (Fig. 2). Cheralite $CaTh(PO_4)_2$ does not show any phase transition at high temperature or high pressure [44].

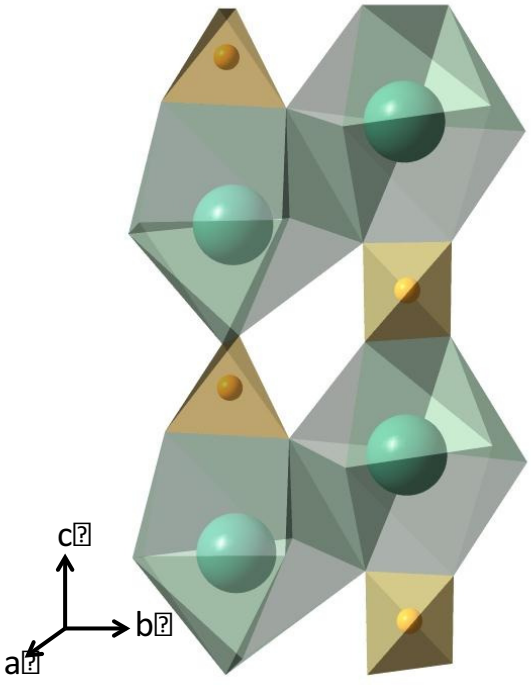

Fig. 2. Polyhedra arrangement in the cheralite structure

Based on steric considerations, Podor *et al.* established the criteria of the stability of $M^{II}M'^{IV}(PO_4)_2$ compounds in the cheralite form (the following limits are different from those reported by the authors since they were recalculated according to r_c instead of r_i) [28]:

. (in Å) (1)

$$^{IX}r(M^{II}) / {}^{IX}r(M'^{IV}) \leq 1.22 \quad (2)$$

This means that cheralite with the $M^{II}M'^{IV}(PO_4)_2$ composition can only be obtained with big tetravalent elements, *i.e.* actinide elements. According to Eq. (1), $CaPu(PO_4)_2$ should not crystallize in the cheralite structure. Unfortunately, this has not been demonstrated yet because of the strong unstability of tetravalent plutonium in the presence of PO_4^{3-} units [45,46]. Note that the incorporation of Pu^{IV} suggested by Tabuteau *et al.* in the proposed $(Ca,Np,Pu)PO_4$ compound can not definitively exclude the presence of Pu^{III} in the structure. Indeed this compound was only characterized by powder XRD, which is not an appropriate technique for the determination of the valence state of a given element [33].

The existence of the mineral yavapaiite was first reported by Hutton in 1959 [47]. The crystal structure was then established by Graeber and Rosenzweig in 1971 on the archetype $KFe(SO_4)_2$, which crystallizes in the $C2/m$ monoclinic space group ($Z = 2$) [48,49]. The yavapaiite layered structure exhibits close relationship with the three-dimensional framework of β-cristobalite, α-$NaTiP_2O_7$, and $CsMoOP_2O_7$ [31]. It consists of layers running parallel to the (001) plane built up of corner-connected $M'O_6$ octahedra and PO_4 tetrahedra. One vertice of each tetrahedron points into the interlayer where the divalent cation M takes place, in a ten-fold oxygen environment (Fig. 3).

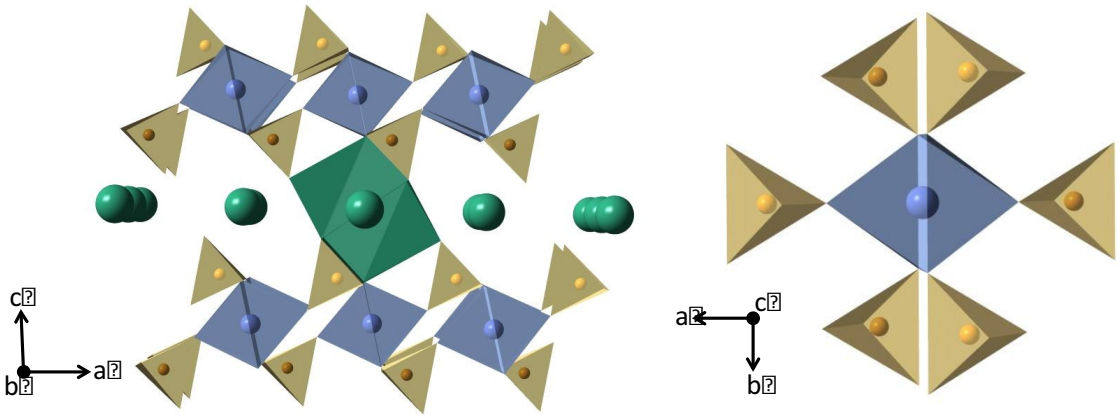

Fig. 3. Yavapaiite structure (left) and corner connection between PO_4 and $M'O_6$ polyhedra (right)

Two structures stem from the yavapaiite one at room temperature, namely "low-yavapaiite" for small cations *M* and *M'* (Ca to Sr and Ge to Zr, respectively). In the frame of the present work, we also propose to name "super-yavapaiite" those made of cations big enough (*i.e.* barium actinide phosphates) to form polyhedra of higher coordination. In contrast with the yavapaiite-type compounds, low-yavapaiite phosphates crystallize in the *C*2/*c* space group. This structure can be described as a distorted yavapaiite with a double lattice along the *a*-axis. Apinitis and Sedmalis reported $PbGe(PO_4)_2$ as the first phosphate with a doubled-lattice yavapaiite derivate structure [35]. Compared to yavapaiite, the tetravalent cation remains in an octahedral environment whereas the divalent cation coordination decreases to eight (capped with 2 additional oxygen atoms). More recently, Zhao *et al.* indexed the room temperature phase of $SrTi(PO_4)_2$ and $SrSn(PO_4)_2$ compounds in the low-yavapaiite *C*2/*c* space group, in contradiction with Paques-Ledent and Keller reports [29,50,51]. Our experiments confirmed the results of Zhao *et al.* We found that the reports of Paques-Ledent and Keller are also erroneous for $SrGe(PO_4)_2$ compound, which crystallizes in the low-yavapaiite structure at room temperature and turns into the yavapaiite *C*2/*m* form at 468 K [52].

The super-yavapaiite compound also crystallizes in the *C*2/*c* space group. The archetype for these compounds is $RbEu(SO_4)_2$ [53]. The structure is made of (100) layers of $M^{II}O_{14}$ polyhedra alternating with dense slabs of $M'^{IV}O_8$ square-based antiprisms and PO_4 tetrahedra. The uncommon $M^{II}O_{14}$ units are distorted elongated hexagonal bipyramids. The high level of coordination of the two cations is consistent with their big size [18].

The existence of two very different structures, cheralite and yavapaiite, stems from the difference of ionic radii of the *M* and *M'* cations, as already suggested by Podor *et al.* and confirmed by the plot of $r(M^{II})$ *vs* $r(M^{IV})$ (Fig. 1) [28]. The high ratio between the ionic radii of the divalent and tetravalent cations in yavapaiite forms results in the ordering of these cations into well-differentiated polyhedra, typically a large one for M^{II} and a small one for M^{IV}. It is worth to note that the cheralite structure is the only non-ordered structure in the $M^{II}M'^{IV}(PO_4)_2$ compounds.

3.2. Other structures

The structures mentioned above cannot describe all the forms encountered for the $M^{II}M'^{IV}(PO_4)_2$ compounds. The high-temperature phase of the $BaM^{IV}(PO_4)_2$ (M^{IV}= Ti, Zr, Hf and Sn), mentioned for the first time by Fukuda *et al.* and described by Bregiroux *et al.* by *ab initio* Rietveld analysis from synchrotron X-ray powder diffraction data is lamellar (denoted as β-phase, or high-yavapaiite), and might also be regarded as derived from the yavapaiite one [10,54]. The archetype for this structure is $KAl(MoO_4)_2$ [55,56]. The (001) layers consist in $M^{IV}O_6$ octahedra sharing corners with PO_4 tetrahedra. The main difference with yavapaiite consists in the fact that faces of polyhedra lie parallel to the (001) plane. This yields the highest possible symmetry of the layers, and barium increases the coordination number from ten to twelve. BaO_{12} and $M^{IV}O_6$ polyhedra are faces-connected, in contrast with yavapaiite, where BaO_{10} and $M^{IV}O_6$ polyhedra only share edges. The phase transition appears as a

topotactic modification of the monoclinic lamellar yavapaiite structure into a trigonal one (S.G. *P*-3*m*1) through a simple mechanism involving the unfolding of the $\left[M(PO_4)_2\right]_n^{2-}$ layers. The transformation of the yavapaiite structure to its high temperature form is found to occur at 747 K and 1604 K, for $BaZr(PO_4)_2$ and $BaSn(PO_4)_2$, respectively.

Note that on the basis of the International Tables for Crystallography [57] and the evident kinship of the lattices and structures, the low-, medium- and high yavapaiite forms are related by the following vectorial equations: the *C*2/*c* (*Z* = 4) low-form (L) is a subgroup of the *C*2/*m* (*Z* = 2) medium-form (M), with $a_L = 2\ c_M$; $b_L = -b_M$; $c_L = a_M$; in turn, the *C*2/*m* medium-form is a subgroup of the *P*-3*m*1 (*Z* = 1) high-form (H), with $a_M = 2\ a_H + b_H$; $b_M = b_H$; $c_M = c_H$.

$PbSn(PO_4)_2$ is also a yavapaiite derivate with a $[Sn(PO_4)_2]^{2-}$ skeleton built of corner-linked SnO_6 octahedra and PO_4 tetrahedra, while lead is located in double tunnels but not in sheets (Fig. 4) [9]. This original structure was explained by the Pb^{II} active lone pair effect, which also conducts to the modification of the lead coordination number to nine.

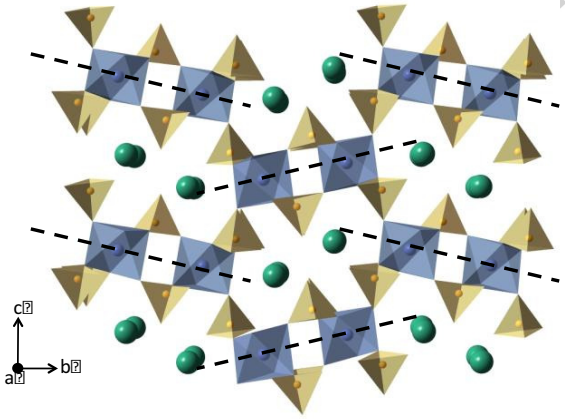

Fig. 4. Crystal structure of $PbSn(PO_4)_2$ (the dashed lines highlight the original layers in the yavapaiite structure)

The structure of $CaZr(PO_4)_2$ was firstly found to be orthorhombic by Fukuda *et al* (S.G. $P2_12_12_1$ *Z* = 4) [24]. Recently, Bregiroux *et al.* revised the crystal structure and found

that $CaZr(PO_4)_2$ actually crystallizes in the orthorhombic space group $Pna2_1$ ($Z = 4$) [58]. The coordination number of both cations is seven. ZrO_7 distorted pentagonal bipyramidal polyhedra share edges with CaO_7 polyhedra and PO_4 tetrahedra forming infinite chains along [010] direction of $[CaO_3ZrO_3(PO_4)_2]^{12-}$ composition. This is a non-layered structure that does not show any structural link with the yavapaiite one, probably because the ionic radius of Zr and Ca are not different enough, which allows to alternate Ca and Zr polyhedral in the same plan (Fig. 5). High temperature XRD analysis highlighted the existence of a high temperature form, very similar to the room temperature one, but more symmetrical (*Pnma*, $Z = 4$).

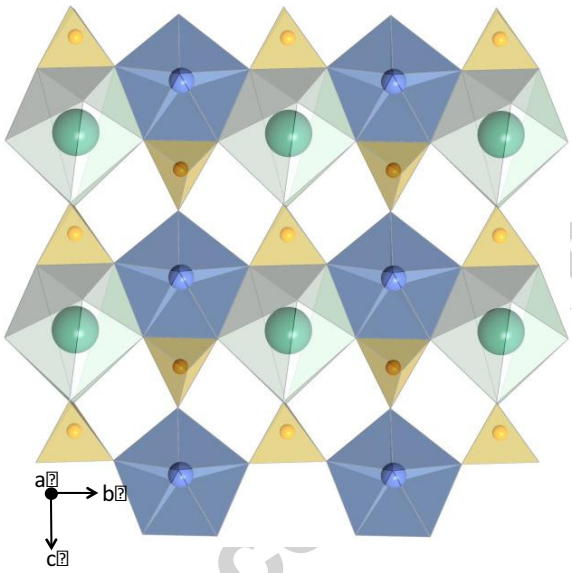

Fig. 5. (100) layer in the orthorhombic $CaZr(PO_4)_2$ structure

$SrZr(PO_4)_2$ shows a particular behavior. At room temperature, $SrZr(PO_4)_2$ is a layered triclinic compound (S.G. *P*-1) containing ZrO_7 distorted pentagonal bipyramidal polyhedra [59]. Due to the high ionic radius of strontium, this latter is ninefold coordinated (actually 8+1 neighbors). The crystal structure of this compound thus consists in four types of polyhedra: ZrO_7, SrO_9 and two different PO_4 tetrahedra (Fig. 6). Two of the ZrO_7 polyhedra share edges and are connected through the two different PO_4 tetrahedra to form infinite chains along [001]

direction. Chains are linked together with formation of sheets with (100) orientation. The thermal behavior analysis of $SrZr(PO_4)_2$ revealed two reversible phase transitions. At 405 K, the structure changes from triclinic to the monoclinic yavapaiite form (*C*2/*m*). Between 1175 K and 1196 K, Fukuda *et al.* found that the structure turned into a hexagonal or trigonal form. According to our previous work on the thermal behavior of the yavapaiite structure, one can suppose that the high temperature form of $SrZr(PO_4)_2$ is the so-called high-yavapaiite structure (*P*-3*m*1) [54]. During these transformations the coordination of the Sr^{II} and Zr^{IV} changes as follows: 9→10→12 and 7→6→6, respectively.

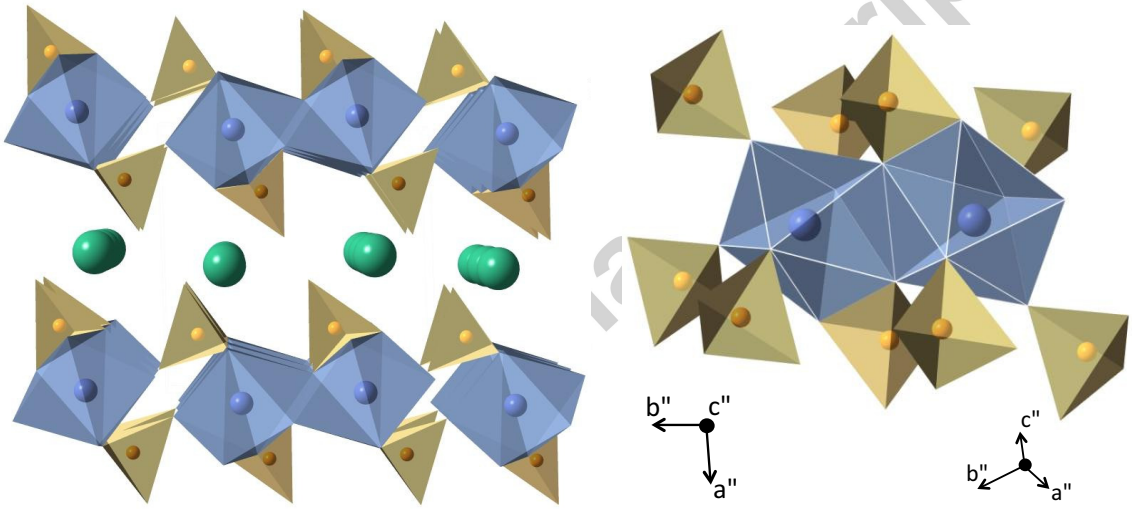

Fig. 6. Room temperature structure of $SrZr(PO_4)_2$

$SrNp(PO_4)_2$ crystallizes in the orthorhombic space group *Cmca*. Though this structure presents alternate layers of SrO_{10} and NpO_8 polyhedra, like in yavapaiite, it is most strongly linked to the cheralite form [22]. The difference in size between Sr^{II} and Np^{IV} is the driving force that orders the cations in $SrNp(PO_4)_2$. It is worth to note that the structure of $SrNp(PO_4)_2$ confirms the position of the border between ordered cheralite and other structures domains defined by Podor *et al.* at a ratio value of $r(M^{II})/r(M'^{IV}) = 1.22$ [28].

Under ambient pressure, $CaU(PO_4)_2$ crystallizes in the non-ordered cheralite form. Dusausoy *et al.* showed that when synthesized at 973 K and 200 MPa, this compound could also be obtained in a xenotime derivate ordered structure [26]. The symmetry is orthorhombic and the space group is *Pnma*. Over 973 K, the structure turns into the cheralite form. This transformation is irreversible and associated to an increase of the compactness of the compound.

3.3. Uncompleted or doubtful structures

Kitaev *et al.* claimed to have obtained $M^{II}Ce^{IV}(PO_4)_2$ (M^{II}= Mg, Ca, Sr, Ba, and Cd) with the cheralite structure under 1073 K [60]. These results are very surprising since it has been demonstrated several times that Ce^{IV} is almost fully reduced into Ce^{III} at high temperature in the presence of phosphates [17,61-63]. Moreover, the cell parameters of the $M^{II}_xCe^{III}_{1-2x}Ce^{IV}_x(PO_4)_2$ compounds given by Kitaev *et al.* are all close to those of $Ce^{III}PO_4$, evidencing a negligible incorporation of M^{II}/Ce^{IV} couple in the cheralite structure ($x \approx 0$) [1].

$BaU(PO_4)_2$ was reported by several authors but the crystal data are still unknown. Nevertheless, according to our previous work on $BaTh(PO_4)_2$ and $BaNp(PO_4)_2$, $BaU(PO_4)_2$ probably crystallizes in the *C*2/*c* super-yavapaiite structure [18].

$MgTh(PO_4)_2$, $MgU(PO_4)_2$ and $SrU(PO_4)_2$ were described as cheralite compounds by Kitaev *et al.*, but the author pointed out that systematic extra peaks on XRD patterns cannot be indexed, suggesting that the structure does not belong to the cheralite structure [60]. Our tries to synthesize $MgM'^{IV}(PO_4)_2$ always led to NASICON-type compounds $Mg_{0,5}M'^{IV}_2(PO_4)_3$. This could be explained by the small size of Mg and the high stability of the NASICON-type structure.

Grosskreutz *et al.* obtained $PbZr(PO_4)_2$ by crystal growth at 1673 K for 20 h under air [30]. This compound seems to crystallize in the orthorhombic system. We tried to obtain it by a high temperature solid-state reaction between PbO, ZrO_2 (or HfO_2) and $NH_4H_2PO_4$. According to chemical analysis, the resulting compound have the expected ratio Pb/Zr(Hf)/P = 1/1/2, but the crystal structure remains unsolved.

3.4. Iso- and heterovalent substitutions in the $M^{II}M'^{IV}(PO_4)_2$compounds

Complete monazite-cheralite solid solutions were obtained and well-characterized several times by different authors: $CePO_4$-$CaTh(PO_4)_2$, $LaPO_4$-$CaTh(PO_4)_2$ and $LnPO_4$-$CaTh(PO_4)_2$-$CaU(PO_4)_2$ (with *Ln* = La, Nd, Gd) [28,34,63]. Based on X-ray powder diffraction and drop calorimetry, Konings *et al.* highlighted that $Ln_{1-2x}Ca_xTh_xPO_4$ solid solutions show deviation from ideal behavior due to lattice strains induced by ion size effects of substitution of Ln^{3+} with $½(Ca^{2+}+Th^{4+})$ [65].

Pepin *et al.* tried to synthesize $Ce^{III}_{1-2x}Ce^{IV}_xM^{II}_xPO_4$ solid solution with M^{II} = Ba and Sr. They showed that Ce^{IV} incorporation into the cheralite structure is very low ($x < 0.1$) [66]. Bregiroux *et al.* demonstrated that the formation of $Ca_{0.5}Ce_{0.5}PO_4$ appears impossible, as well as $Ca_{0.5}Pu^{IV}_{0.5}PO_4$, due to the important reduction of Ce^{IV} into Ce^{III} above 1113 K [61]. Recently, Asuvathraman and Kutty published results on $Ca_{0.2}Ce_{0.8}PO_4$ compounds with the monazite structure [66]. A rigorous analysis of their XRD patterns reveals the presence of traces of $Ca_2P_2O_7$ in their compounds. Although the presence of Ce^{IV} seems to be confirmed by XPS analysis, the weight loss observed at high temperature by thermogravimetry of the precursor of $Ca_{0.2}Ce_{0.8}PO_4$ confirms the reduction of a large amount of cerium. These results confirm that the incorporation of a divalent cation in cerium-based monazite is very weak due

to the high tendency of Ce^{IV} to reduce in phosphate environment, as previously observed by Bregiroux *et al.* [61].

Deschanels *et al.* synthesized the compound $Ca_{0.18}Th_{0.18}Pu_{0.18}La_{1.46}(PO_4)_2$ in which Pu is exclusively in its trivalent form [67]. Tabuteau *et al.* showed that tetravalent plutonium can be incorporated in $CaNp_{1-x}Pu_x(PO_4)_2$ within the limit of x = 0.3 [33]. Nevertheless, as already mentioned, due to the lack of appropriate characterizations, the presence of Pu(III) in this compound can not be excluded. Bregiroux *et al.*, who obtained $Pu_{0.4}^{III}Pu_{0.3}^{IV}Ca_{0.3}^{II}PO_4$ samples, confirmed the instability of tetravalent plutonium in the cheralite structure [45].

The $BaHf_{1-x}Zr_x(PO_4)_2$ solid-solution was studied by Miao and Torardi [12]. Surprisingly, despite the fact that the end-members structure is identical and the ionic radii of Zr^{IV} and Hf^{IV} very close, they found that the pure phase can only be obtained for x < 0.2. The authors also tried to prepare $Ba_{1-y}Eu^{II}_yHf(PO_4)_2$ (y < 0.03) by two steps: firing in air at 373 K for 12 h following by another treatment at 1173 K under 2 % H_2 in argon. Optical characterization only showed the Eu^{3+} red emission and the authors could not prove whether Eu entered the yavapaiite structure or not.

Fukuda *et al.* analyzed $Ba_{1-x}Sr_xZr(PO_4)_2$ compounds and obtained different structures, depending of x. [38]. Yavapaiite structure is only obtained for $x \leq 0.1$. For $0.2 \leq x \leq 0.7$, the authors found a yavapaiite superstructure along *a* (double cell), in the monoclinic *P*2/*c* space group. When heated, this structure turns into the yavapaiite form and then into the trigonal high-yavapaiite one. For $0.8 \leq x \leq 0.9$, a mixture of the superstructure and the triclinic structure already described below is obtained.

$Ce_{2-2x}Ba_xM'^{IV}_x(PO_4)_2$ (M'^{IV}= Zr, Hf) cheralite-like compounds were succesfully synthesized by solid state reaction by Popa *et al.*, for x ≤ 0.2, evidencing a low solubility of yavapaiite-building cations in the cheralite structure [5]. This result is consistent with that obtained by

Montel *et al.* who found that $La_{2-2x}Ba_xTh_x(PO_4)_2$ can be obtained in the cheralite form only for $x < 0.5$ [25]. The solubility of monazite-forming La^{III} in $BaTh(PO_4)_2$ was not investigated.

5. Properties

5.1. Behavior of $M^{II}M'^{IV}(PO_4)_2$ compounds in nuclear context

Cheralite compounds $CaAn(PO_4)_2$ (*An* = Th, U, Np, Pu) were intensively studied during the last twenty years as promising candidates for the specific immobilization of highly radioactive actinides elements (Pu, Np and Cm), since they can accept within their structure high amounts of such elements, while maintaining good resistance to aqueous alteration and to radiation damages. Moreover, U- and Th-cheralite and cheralite/monazite solid solutions can be sintered at lower temperature compared to pure monazite ceramics [8,69-79].

Recently, $M^{II}M'^{IV}(PO_4)_2$ compounds showed a strong interest in the field of used fuel recycling since the radiolysis of the solutions obtained by reaction with tributyl phosphate (TBP) induces the precipitation of phosphate compounds containing both fission products (Cs, Sr, Ba, Pb, Mo, W, Zr…) and actinides [14].

As potential candidates for the specific immobilization of long-life radionuclides, the chemical durability of cheralite compounds were extensively studied [80,81]. These compounds show high chemical durability, with normalized dissolution rate as low as $2.2 \pm 0.2\ 10^{-5}$ $g.m^{-2}.day^{-1}$ in dynamic conditions at 363 K in 10^{-1} M HNO_3 for $Ca_{0.5}Th_{0.5}PO_4$ and $9.7 \pm 0.8\ 10^{-5}$ $g.m^{-2}.day^{-1}$ at 343 K in 10^{-1} M HNO_3 for $Ca_{0.5}Th_{0.4}U_{0.1}PO_4$ [82]. This very good chemical durability of cheralite/monazite solid solution can be explained its compact structure and the absence of open channel like, for instance, in britholite compounds $Ca_9Nd(PO_4)_5SiO_4F_2$. The degradation of the chemical durability induced by the presence of

tetravalent uranium is explained by its tendency to oxidize at the solid-liquid interface during the dissolution process.

Th/U bearing cheralite compounds were known to show very interesting behavior under self-irradiation. As observed for other phosphate – based ceramics like β-PDT or britholite, the behavior of cheralite under irradiation is governed by two opposite effects: creation of structural defects by alpha particles and self-annealing at relatively low temperature [74,75]. Thus, the cheralite structure remains crystalline as long as the creation of defects is entirely compensated by self-annealing. Indeed, well-crystallized 2 billion years aged (U,Th)-cheralite natural samples were discovered [70].

5.2. Thermal expansion

Because of the anisotropy of the crystal structure, yavapaiite and derived compounds show a strongly anisotropic thermal expansion [10,54]. Bregiroux *et al.* analyzed the expansion mechanism of room temperature and high temperature forms of $BaZr(PO_4)_2$. In the yavapaiite form, the thermal expansion consists in the unfolding of the $[Zr(PO_4)_2]_n^{2-}$ layers, involving various phenomena such as bridging oxygen rocking motion in the Zr-O-P linkage. The resulting cell parameters thermal expansion are 34.0, -4.1 and 7.3 10^{-6} K^{-1} for *a*, *b* and *c*, respectively. In the high temperature form, the unfolded $[Zr(PO_4)_2]_n^{2-}$ layers cannot expand any more, so that the crystal structure only expands along the c-axis. In their recent work, Bregiroux *et al.* showed that $CaZr(PO_4)_2$ exhibits a quite low, but also isotropic, linear thermal expansion coefficient of 6.11 10^{-6} K^{-1} [58]. On the opposite, lanthanide monophosphates with the monazite structure, show almost isotropic thermal expansion in the range of 9 to 10 10^{-6} K^{-1} [83].

5.3. Optical properties

Several authors highlighted interesting optical properties for $M^{II}M'^{IV}(PO_4)_2$ compounds. $BaTi(PO_4)_2$ shows a yellow photoluminescence below 100 K due to titanate octahedra [11]. $PbGe(PO_4)_2$ is a green emitter at room temperature when excited by UV irradiation [35]. According to Miao and Torardi, $BaHf_{1-x}Zr_x(PO_4)_2$ solid solutions (x = 0 – 0.2) are UV-emitting phosphors under X-ray excitation at room temperature. The high efficiency of these phosphors makes them good candidates for use in medical diagnostic imaging systems [12]. The authors also tried to dope the latter compound by divalent Eu in order to shift the emission band toward the blue region, but emission spectra were identical before and after calcination under H_2/Ar atmosphere. Considering the ionic radius of Ba^{2+} and Eu^{2+} and the fact that Eu^{2+} can easily substitute for Ba^{2+} in $BaMgAl_{10}O_{17}:Eu^{2+}$ (BAM) phosphors, this result was unexpected [84]. Nevertheless, our own tries to dope yavapaiite compounds by Eu^{2+} were also unsuccessful. Red, green and blue emitting phosphors when energized with X-ray and VUV-UV were obtained by Zhang *et al.* by doping $CaZr(PO_4)_2$ by Eu^{3+}, Tb^{3+} and Tm^{3+}, respectively [13]. Zhang *et al.* reported that $CaZr(PO_4)_2$ compounds exhibit elastic-mechanoluminescence properties when doped with divalent europium Eu^{2+} [85]. The same team prepared mixed-valence Eu-doped $CaZr(PO_4)_2$ compounds as tunable white light emitting deep UV LEDs [86]. The authors explained the reduction mechanism of Eu^{3+} to Eu^{2+} in air at high temperature by a charge compensation model. This phenomenon was already observed in $Ba_3(PO_4)_2$:Eu [87]. $PbGe(PO_4)_2$ was found to be an intrinsic green emitting phosphor. When doped with red-emitting Eu^{3+} ion, this color can be tuned from blue-green to white [35].

5.4. Dielectric properties

A recent work detailed the dielectric properties of ten ceramics in the $M^{II}M'^{IV}(PO_4)_2$ family [88]. Yavapaiite compounds were found to be faint ionic conductors. On the other hand, $SrGe(PO_4)_2$, $BaGe(PO_4)_2$, $CaZr(PO_4)_2$, $BaZr(PO_4)_2$, and $BaSn(PO_4)_2$ showed excellent dielectric characteristics (small losses around 3 – 6 % and permittivity values of 2.29 – 8.02) that make them promising materials for use in microwave applications.

Conclusions

$M^{II}M'^{IV}(PO_4)_2$ compounds find numerous applications in different fields, such as nuclear, optical, dielectric materials… Their crystal structures have been reviewed according to the cations size. $M^{II}M'^{IV}(PO_4)_2$ structures stem from two different archetypes: the cheralite and the yavapaiite structures, with some exceptions. To date, structures of some end members remain unknown. Moreover, this review highlights that solid solutions could exhibit particular behavior, justifying the in-depth investigation of their crystal structure. Finally, the thermal behavior, especially the potential phase transition, has not been explored yet for some compositions, *e.g.* $PbSn(PO_4)_2$.

Acknowledgements

K.P. acknowledges La Mairie de Paris for the ‘‘Research in Paris’’ 2010-2011 fellowship.

References

[1] N. Clavier, R. Podor, N. Dacheux, J. Eur. Ceram. Soc. 31 (2011) 941-976;

[2] I.V. Tananaev (Ed.), The Chemistry of Tetravalent Elements Phosphates, Nauka, Moscow, 1972;

[3] A. Durif, Crystal chemistry of condensed phosphates, Plenum Press, New York, London, 1995;

[4] K. Popa, R.J.M. Konings, P. Boulet, D. Bouëxière, A.F. Popa, Thermochim. Acta 436 (2005) 51-55;

[5] K. Popa, H. Leiste, T. Wiss, R.J.M. Konings, J. Radioanal. Nucl. Chem. 273 (2007) 563-56;

[6] A.J. Locock, Crystal chemistry of actinide phosphates and arsenates, in: S.V. Krivovichev, P.C. Burns, I.G. Tananaev (Eds.), Structural chemistry of inorganic actinide compounds, Elsevier B.V., Amsterdam, 2007, pp. 217-278;

[7] A.I. Orlova, Crystal and structural chemistry of anhydrous tri- and tetravalent actinide orthophosphates, in: S.V. Krivovichev, P.C. Burns, I.G. Tananaev (Eds.), Structural chemistry of inorganic actinide compounds, Elsevier B.V., Amsterdam, 2007, pp. 315-340;

[8] N. Dacheux, N. Clavier, R. Podor, Am. Miner. 98 (2013) 833-847;

[9] E. Morin, G. Wallez, S. Jaulmes, J.C. Couturier, M. Quarton, J. Solid State Chem. 137 (1998) 283-288;

[10] K. Fukuda, A. Moriyama, T. Iwata, J. Solid State Chem. 178 (2005) 2144-2151;

[11] G. Blasse, G.J. Dirksen, Chem. Phys. Lett. 62 (1979) 19-20;

[12] C.R. Miao, C.C. Torardi, J. Solid State Chem. 155 (2000) 229-232;

[13] Z.J. Zhang, J.L. Yuan, X.J. Wang, D.B. Xiong, H.H. Chen, J.T. Zhao, Y.B. Fu, Z.M. Qi, G.B. Zhang, C.S. Shi, J. Phys. D: Appl. Phys. 40 (2007) 1910-1914;

[14] L.R Morss, N. Edelstein, J. Fuger, J.J. Katz (Eds.), The Chemistry of the Actinide and Transactinide Elements (Set Vol.1-6), fourth ed., Springer Netherlands, 2011;

[15] V. Brandel, N. Dacheux, J. Solid. State Chem. 177 (2004) 4743-4754;

[16] V. Brandel, N. Dacheux, J. Solid State Chem. 177 (2004) 4755-4767;

[17] K. Popa, D. Bregiroux, R.J.M. Konings, T. Gouder, A.F. Popa, T. Geisler, P.E. Raison, J. Solid State Chem. 180 (2007) 2346-2355;

[18] G. Wallez, D. Bregiroux, K. Popa, P.E. Raison, C. Apostolidis, P. Lindqvist-Reis, R.J.M. Konings, A.F. Popa, Eur. J. Inorg. Chem. (2011) 110-115;

[19] K. Popa, R.J.M. Konings, O. Beneš, T. Geisler, A.F. Popa, Thermochim. Acta 451 (2006) 1-4;

[20] P.E. Raison, R. Jardin, D. Bouëxière, R.J.M. Konings, T. Geisler, C.C. Pavel, J. Rebizant, K. Popa, Phys. Chem. Minerals 35 (2008) 603-609;

[21] K. Popa, T. Shvareva, L. Mazeina, E. Colineau, F. Wastin, R.J.M. Konings, A. Navrotsky, Amer. Miner. 93 (2008) 1356-1362;

[22] K. Popa, G. Wallez, P.E. Raison, D. Bregiroux, C. Apostolidis, P. Lindqvist-Reis, R.J.M. Konings, Inorg. Chem. 49 (2010) 6904-6908;

[23] G. Wallez, N. Clavier, N. Dacheux, M. Quarton, W. van Beek, J. Solid State Chem. 179 (2006) 3007-3016;

[24] K. Fukuda, K. Fukutani, Powder Diffr. 18 (2003) 296-300;

[25] J.-M. Montel, J.-L. Devidal, D. Avignant, Chem. Geol. 191 (2002) 89-104;

[26] Y. Dusausoy, N.E Ghermani, R. Podor, M. Cuney, Eur. J. Mineral. 8 (1996) 667-673;

[27] R. Podor, M. Cuney, C.N. Trung, Am. Mineral. 80 (1995) 1261-1268;

[28] R. Podor, M. Cuney, Am. Mineral. 82 (1997) 765-771;

[29] D. Zhao, H. Zhang, Z. Xie, W.-L. Zhang, S.-L. Yang, W.-D. Cheng, Dalton Trans. (2009) 5310-5318;

[30] W. Groskreutz, W. Wieker, Z. Chem. 18 (1978) 349 (in german);

[31] A. Leclaire, M.M. Borel, J. Chardon, B. Raveau, J. Solid State Chem. 116 (1995) 364-368;

[32] R. Masse, A. Durif, C.R. Acad. Sc. Paris 274 (1972) 1692-1695;

[33] A. Tabuteau, M. Pagès, J. Livet, C. Musikas, J. Mater. Sci. Lett. 7 (1988) 1315-1317;

[34] O. Terra, N. Dacheux, N. Clavier, R. Podor, F. Audubert, J. Am. Ceram. Soc. 91 (2008) 3673-3682;

[35] W.-L. Zhang, C.-S. Lin, Z.-Z. He, H. Zhang, Z.-Z. Luo, W.-D. Cheng, CrystEngComm 15 (2013) 7089-7094;

[36] S. Apinitis, U. Sedmalis, Izvestia Akademii Nauk Latvijskoj SSR. Seria Himiceskaa 6 (1984) 643-645;

[37] M. Keskar, R. Phatak, S.M. Sali, K. Krishnan, N.D. Dahale, N.K. Kulkarni, S. Kannan, J. Nucl. Mater. 409 (2011) 9-17;

[38] K. Fukuda, T. Iwata, A. Moriyama, S. Hashimoto, J. Solid State Chem. 179 (2006) 3870-3876;

[39] R.D. Shannon, Acta Crystallogr. A32 (1976) 751-767;

[40] S.H.U. Bowie, J.E.T. Horne, Mineral. Mag. 30 (1953) 93-99;

[41] D. Rose, Neues. Jahrb. Mineral. Monatsh. 6 (1980) 247-257;

[42] K. Linthout, Can. Mineral. 45 (2007) 503-508;

[43] G.W. Beall, L.A. Boatner, D.F. Mullica, W.O. Milligan, J. Inorg. Nucl. Chem. 43 (1981) 101-105;

[44] P.E. Raison, S. Heathman, G. Wallez, C.E. Zvoriste, D. Bykov, G. Ménard, E. Suard, K. Popa, N. Dacheux, R.J.M. Konings, R. Caciuffo, Phys. Chem. Miner. 39 (2012) 685-692;

[45] D. Bregiroux, R. Belin, P. Valenza, F. Audubert, D. Bernache-Assollant, J. Nucl. Mater. 366 (2007) 52-57;

[46] N. Dacheux, R. Podor, V. Brandel, M. Genet, J. Nucl. Mater. 252 (1998) 179-186;

[47] C.O. Hutton, Am. Miner. 44 (1959) 1105-1114;

[48] E.J. Graeber, A. Rosenzweig, Am. Miner. 56 (1971) 1917-1933;

[49] J.W. Anthony, W.J. McLean, Am. Miner. 57 (1972) 1546-1549;

[50] M.T. Paques-Ledent, J. Inorg. Nucl. Chem. 39 (1977) 11-17;

[51] L.P. Keller, G.J. McCarthy, ICDD Grant-in-Aid, JCPDS File no. 33-150, North Dakota State University, Fargo, North Dakota, USA, 1982;

[52] K. Popa, G. Wallez, D. Bregiroux, P. Loiseau, J. Solid State Chem. 184 (2011) 2629-2634;

[53] N.L. Sarukhanyan, L.D. Iskhakova, V.K. Trunov, Sov. Phys. Crystallogr. 28 (1983) 266-268;

[54] D. Bregiroux, K. Popa, R. Jardin, P.E. Raison, G. Wallez, M. Quarton, M. Brunelli, C. Ferrero, R. Caciuffo, J. Solid State Chem. 182 (2009) 1115-1120;

[55] R.F. Klevtsova, P.V. Klevtsov, Kristallografiya 15 (1970) 953-959;

[56] S. Oyetola, A. Verbaere, Y. Piffard, M. Tournoux, Eur. J. Solid State Inorg. Chem. 25 (1988) 259-278;

[57] International Tables for Crystallography, Vol. A. space-group symmetry, D. Reidel Publ. Co., Dordrecht, Holland/Boston, U. S. A., 1983;

[58] D. Bregiroux, G. Wallez, K. Popa, Solid State Sci. 41 (2015) 43-47;

[59] K. Fukuda, A. Moriyama, S. Hashimoto, J. Solid State Chem. 177 (2004) 3514-3521;

[60] D.B. Kitaev, Y.F. Volkov, A.I. Orlova, Radiochemistry 46 (2004) 211-217;

[61] D. Bregiroux, O. Terra, F. Audubert, N. Dacheux, V. Serin, R. Podor,D. Bernache-Assollant, Inorg. Chem. 46 (2007) 10372-10382;

[62] A. Borhan, B. Apetrachioaei, K. Popa, Rev. Roum. Chim. 55 (2010) 389-393;

[63] R. Heindl, E. Flemke, J. Loriers, Conf. Dig. Inst. Phys.(1971), 222-224;

[64] Y. Hikichi, K. Hukuo, J. Shiokawa, Nippon Kagaku Kaishi, 12 (1978) 1635-1640 (in japanese);

[65] R.J.M. Konings, M. Walter, K. Popa, J. Chem. Thermodynamics, 40 (2008) 1305-1308;

[66] J.G. Pepin, E.R. Vance, G.J. McCarthy, Mat. Res. Bull. 16 (1981) 627-633;

[67] R. Asuvathraman, K.V. Govindan Kutty, Thermochim. Acta, 581 (2014) 54-61;

[68] X. Deschanels, V. Picot, B. Glorieux, F. Jorion, S. Peuget, D. Roudil, C. Jégou, V. Broudic, J.N. Cachia, T. Advocat, C. Den Auwer, C. Fillet, J.P. Coutures, C. Henning, A. Scheinost, J. Nucl. Mater. 352 (2006) 233-240;

[69] W.C. Overstreet, U.S. Geological Survey Professional Paper 530 (1967) 1-327;

[70] C.M. Gramaccioli, T.V. Segalstad, Am. Mineral. 63 (1978) 757-761;

[71] B.C. Sales, C.W. White, L.A. Boatner, Nucl. Chem. Waste Managem. 4 (1983) 266-268;

[72] L.A. Boatner, G.W. Beall, M.M. Abraham, C.B. Finch, P.G. Hurray, M. Rappaz, p. 289 in Scientific Basis for Nuclear Waste Management, Vol. 2, Edited by C.J.M. Northrup Jr. Material Research Society, Warrendale, PA, USA, New York, 1980;

[73] L.A. Boatner, B.C. Sales, in Radioactive waste forms for the future, Edited by W. Lutze, R.C. Ewing, North Holland, Amsterdam (1988) 495-564;

[74] A. Meldrum, L.A. Boatner, W.J. Weber, R.C. Ewing, Geochim. Cosmochim. Acta 62 (1998) 2509-2520;

[75] X. Deschanels, A.M. Seydoux-Guillaume, V. Magnin, A. Mesbah, M. Tribet, M.P. Moloney, Y. Serruys, S. Peuget, J. Nucl. Mater. 448 (2014) 184-194;

[76] O. Terra, N. Clavier, N. Dacheux, R. Podor, New J. Chem. 27 (2003) 957-967;

[77] R.C. Ewing, Progr. Nucl. Energy 49 (2007) 635-643;

[78] D. Olander, J. Nucl. Mater. 389 (2009) 1-22;

[79] H. Schlenz, J. Heuser, A. Neumann, Z. Kristallogr. 228 (2013) 113-123;

[80] E. Du Fou de Kerdaniel, N. Clavier, N. Dacheux, O. Terra, R. Podor, J. Nucl. Mater. 362 (2007) 451-458;

[81] O. Terra, N. Dacheux, F. Audubert, R. Podor, J. Nucl. Mater. 352 (2006) 224-232;

[82] E. Veilly, E. du Fou de Kerdaniel, J. Roques, N. Dacheux, N. Clavier, Inorg. Chem. 47 (2008) 10971-10979;

[83] L. Perrière, D. Bregiroux, B. Naitali, F. Audubert, E. Champion, D.S. Smith, D. Bernache-Assollant, J. Eur. Ceram. Soc. 27 (2007) 3207-3213;

[84] J. Lambert, G. Wallez, M. Quarton, T. Le Mercier, W. van Beek, J. Lumin. 128 (2008) 366-372;

[85] J.C. Zhang,C.N. Xu, Y.Z. Long, Opt. Express 21 (2013) 13699-13709;

[86] J.C. Zhang, Y.Z. Long, H.D. Zhang, B. Sun, W.P. Han, X.Y. Sun, J. Mater. Chem. C. 2 (2014) 312-318;

[87] I. Tāle, P. Kūlis, V. Kronghauz, J. Lumin. 20 (1979) 343-347;

[88] F. Tudorache, K. Popa, L. Mitoseriu, N. Lupu, D. Bregiroux, G. Wallez, J. Alloys Compd. 509 (2011) 9127-9132;

Highlights

- Crystal structure - composition relationships of $M^{II}M'^{IV}(PO_4)_2$ compounds
- Review of the various processes used for the synthesis of these compounds
- Their most reported properties are described and discussed

In this paper, the relationships between composition and crystal structure of $M^{II}M'^{IV}(PO_4)_2$ compounds are established. A review of the various processes used for the synthesis of these compounds is also proposed, as well as their most reported properties.